Effective Rate Enhancement for RIS-Assisted Systems: An Irregular Element-Grouping Structure

Yansong Bai*†, Liyan Li*†,Yunlong Cai*†, and Minjian Zhao*†
*College of Information Science and Electronic Engineering, Zhejiang University, Hangzhou 310027, China
†Zhejiang Provincial Key Laboratory of Information Processing, Communication and Networking (IPCAN), Hangzhou 310027, China
Emails:{22231103, liyan_li, ylcai, mjzhao}@zju.edu.cn

***Abstract*—This paper studies a wireless communication system assisted by a reconfigurable intelligent surface (RIS). We design a practical communication protocol that considers the time and power required for channel estimation and control feedback. Based on this protocol, we propose a novel irregular element-grouping RIS. By designing the selection topology, elements are irregularly selected from the RIS, providing additional spatial degrees of freedom despite a limited number of elements. To further reduce the overhead associated with channel estimation and control feedback, we employ an element-grouping method. Each group consists of a set of adjacent elements that share the same combined channel and phase shift. To maximize the effective rate (ER), we propose an algorithm that jointly optimizes the selection topology, phase shift design, and transmit power allocation. Numerical results demonstrate that the proposed structure increases the ER by up to 41% and 24% compared to regular RIS and regular RIS with element-grouping, respectively.**

***Index Terms*—Reconfigurable intelligent surface (RIS), element-grouping, irregular design, topology optimization.**

I. Introduction

Reconfigurable intelligent surface (RIS) has attracted great interest due to its benefits, such as enhancing signal quality, extending coverage, and reducing energy consumption [1], [2]. By controlling the phase, amplitude, and polarization of incoming waves, RIS effectively improves system security [3], and reduces communication outages.

Recent studies have explored various optimization metrics. [4] employs gradient descent search and sequential fractional programming to optimize precoding and power allocation to enhance energy efficiency (EE) for multi-user scenarios. By alternately optimizing the phase shifts at the RIS and the active precoding at the base station (BS), [5] maximizes the weighted sum rate in a multi-cell massive multiple-input multiple-output (MIMO) communication system. The transmit power at the BS is minimized using the successive refinement method in [6]. [7] proposes iterative strategies such as fixed-point iteration, manifold optimization, and branch-and-bound methods to maximize the instantaneous SNR.

This work was supported in part by the National Natural Science Foundation of China under Grant U22A2004, and in part by Zhejiang Provincial Key Laboratory of Information Processing, Communication and Networking (IPCAN), Hangzhou 310027, China.

In a classical regular RIS-assisted wireless system, the received power has a quadratic relationship with the number of RIS elements, making the performance highly dependent on the number of these elements. Given the practical constraint of a limited number of RIS elements, enhancing system performance under these conditions is crucial.

In [8], the comparison between the RIS and the decode-and-forward (DF) relaying is studied, and the number of reflecting elements in the RIS-assisted system that can achieve a higher rate than the DF relaying is analyzed. [9] minimizes the number of reflecting elements to ensure that the ratio of the system sum rate to capacity exceeds a predefined threshold. [10] examines the approximate ergodic capacity of an RIS-assisted system with phase errors and analyzes the number of reflecting elements needed to guarantee spectral efficiency (SE) performance.

The aforementioned papers utilize the classical regular RIS to assist communication, where elements are regularly arranged on a grid with a constant inter-element spacing, as shown in Fig. 1. This structure selects all elements, including those with poor channel conditions. Additionally, these studies assume channel state information (CSI) is known and overlook the control feedback process. However, channel estimation and control feedback are crucial for the entire communication process. In the channel estimation phase, user equipment (UE) sends pilot signals to obtain CSI. In the control feedback phase, BS reports the optimized configuration to the RIS. The time and power consumption of these phases cannot be neglected, especially for large-scale RIS [11]. Moreover, these works rely on precise phase control for each element. When the communication cycle duration is limited, this precision compresses the available time for data transmission.

Motivated by these considerations, we propose the irregular element-grouping RIS in this paper. By designing the topology of limited elements, the irregular structure provides extra spatial degrees of freedom. Besides, to reduce the overhead of channel estimation and control feedback, we group adjacent elements based on the channel correlation revealed by [12]. Elements within a group share the same combined channel and phase shift. This element-grouping method further enhances the effective rate (ER) of data transmission and simplifies the complexity of phase shift design.

979-8-3315-2096-0/25/$31.00 ©2025 IEEE

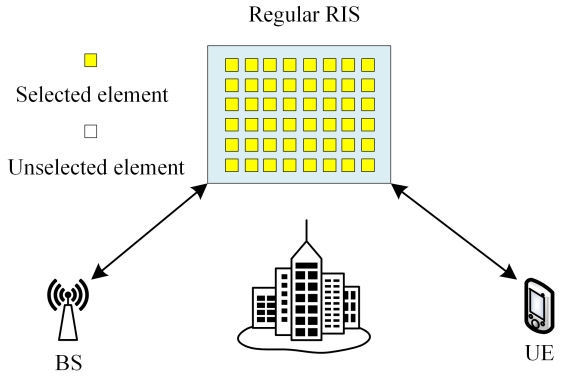

Fig. 1. Regular RIS assisted communication system.

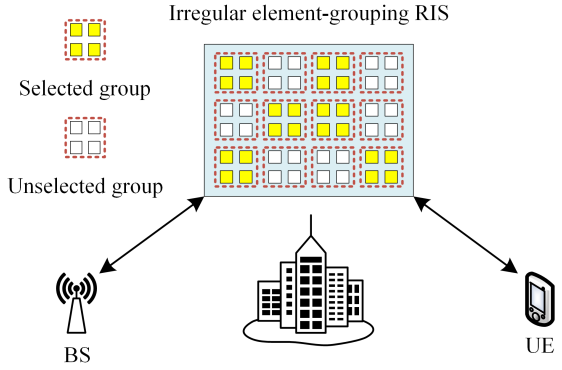

Fig. 2. Irregular element-grouping RIS-assisted communication system.

The rest of this paper is organized as follows. The model of the proposed irregular element-grouping RIS-assisted system is introduced in Section II-A. Then we formulate the ER optimization problem for the proposed system in Section II-B. A joint optimization algorithm is proposed to solve this problem in Section III. Numerical results are shown in Section IV, and the conclusions are drawn in Section V.

II. System Model And Problem Formulation

A. System Model

We consider a single-user communication system assisted by an RIS, as shown in Fig. 2. The BS is equipped with K antennas, and the RIS is composed of N passive reflecting elements. The direct path between the BS and the UE is obstructed. Define $\mathbf{H} = [\mathbf{h}_1, \mathbf{h}_2, \ldots, \mathbf{h}_K] \in \mathbb{C}^{N\times K}$ and $\mathbf{G} = [g_1, g_2, \ldots, g_N] \in \mathbb{C}^{1\times N}$ as the channel matrices from the BS to the RIS and from the RIS to the UE. $\mathbf{h}_k = [h_{1,k}, h_{2,k}, \ldots, h_{N,k}]^T \in \mathbb{C}^{N\times 1}$ represents the channel from the k-th antenna of the BS to the UE. Here we consider the correlated Rayleigh fading channel [12]. Mathematically, the channel is characterized as

$$\mathbf{h}_k \sim \mathcal{CN}(0, \mathbf{R}_N), \tag{1}$$

where $\mathbf{R}_N$ denotes the correlation matrix given by

$$\mathbf{R}_N = \kappa \mathbf{R}, \tag{2}$$

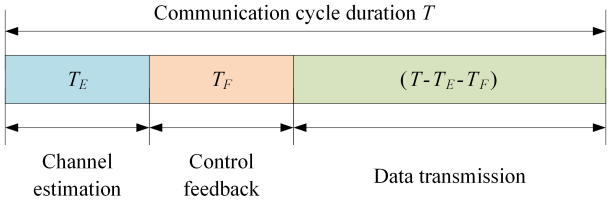

Fig. 3. Proposed transmission protocol.

in which κ is the path loss and the (i,j)-th element of $\mathbf{R}$ is

$$[\mathbf{R}]_{i,j} = \operatorname{sinc}\left(2\left\|\mathbf{u}_i - \mathbf{u}_j\right\|/\lambda\right), i,j = 1,\ldots,N. \tag{3}$$

In (3), $\mathbf{u}_i$ and $\mathbf{u}_j$ represent the position coordinates of the i-th and j-th elements, and λ is the wavelength of the plane wave. Consequently, the channel correlation between RIS elements is determined by spatial distance, making it feasible to group adjacent elements. $\mathbf{G}$ follows the same modeling.

Irregular RIS focuses on the spatial distribution of limited elements. To be specific, the topological structure of the irregular RIS can be designed by selecting N_s viable positions from a set of N grid points. The unselected grid point can be switched off through a diode-based controller [13]. Let $\mathbf{Z} = \operatorname{diag}([z_1, z_2, \ldots, z_N])$ denote the selection topology matrix of the irregular RIS, where $z_n \in \{1, 0\}$. $z_n = 1$ means that the n-th grid point is selected, while $z_n = 0$ means that the n-th grid point is not selected. Define $\rho = N_s/N$ as the ratio of the selected elements.

Define $\mathbf{\Phi} = \operatorname{diag}\left(e^{j\phi_1}, \ldots, e^{j\phi_N}\right)$ as the RIS phase shift matrix. In practical applications, the phase shifts are typically subject to finite discrete constraints. The discrete valued phase shift set is given by $\mathcal{F} = \left\{0, \frac{2\pi}{2^b}, \ldots, \frac{2\pi}{2^b}\left(2^b - 1\right)\right\}$, where b is the number of quantized bits.

Then the signal received by the UE is represented as

$$y = (\mathbf{GZ\Phi Hw})\, x + n, \tag{4}$$

where x represents the normalized transmitted signal at the BS, $\mathbf{w} \in \mathbb{C}^{K\times 1}$ is the beamforming vector of the BS, and n is the additive white Gaussian noise (AWGN). Define N_0 as the noise power spectral density.

We use a practical transmission protocol, as illustrated in Fig. 3. The communication cycle duration T is segmented into three phases: the channel estimation phase T_E, the control feedback phase T_F, and the data transmission phase $(T - T_E - T_F)$. Channel estimation is completed through the uplink, while the other two phases are completed through the downlink. p, p_F, B, and B_F represent the data transmission and control feedback powers and bandwidths, respectively.

Following the model developed in [11], we have $T_E = (NK + 1)/B$ and

$$T_F = \frac{N + N_s b}{B_F \log_2\left(1 + \frac{p_F |h_F|^2}{N_0 B_F}\right)}, \tag{5}$$

where h_F is the feedback channel from the RIS to the BS. In (5), the numerator represents the total number of the control

bits and the denominator is the achievable transmission rate of the control feedback link. Each element requires one bit to switch the "selected/unselected" state, and b bits to configure the phase shift if the element is selected. In the channel estimation phase, the training phase shifts at the RIS are configured based on the discrete Fourier transform (DFT) training scheme proposed in [14], and the channel matrix is estimated by the least squares (LS) estimator.

We assume the BS uses a fixed power p_E for channel estimation. Therefore, the total average power consumption P_{total} only needs to include the other two phases, which is given by

$$P_{total} = \frac{(T - T_E - T_F)}{T}\mu p + \frac{\mu_F p_F T_F}{T}, \tag{6}$$

where μ and μ_F denote the transmit amplifier efficiency. For the sake of simplicity, we set $\mu = \mu_F = 1$.

From the expressions of T_E and T_F, it can be seen that an increase in N will lead to a proportional increase in T_E and T_F. Thus, we propose the element-grouping method. The N elements are uniformly divided into M groups with each group containing $Q = N/M$ elements, and we select $M_s = M\rho$ groups among them. Then T_E and T_F are reduced to about $1/Q$ of their original values. The new phase shift matrix and the selection topology matrix become $\mathbf{\Theta} = \mathrm{diag}\left(\left[e^{j\theta_1}, e^{j\theta_2}, \ldots, e^{j\theta_M}\right]\right)$ and $\mathbf{Z} = [z_1, z_2, \ldots, z_M]$.

After element-grouping and topology design, the irregular element-grouping RIS is shown in Fig. 2. Let $\mathbf{V} \in \mathbb{C}^{M\times K}$ denote all the cascaded channels. The (m,k)-th element of $\mathbf{V}$ is represented as $v_{m,k} = \sum_{j=(m-1)Q+1}^{mQ} h_{j,k} * g_j$. Then the received signal by the UE in (4) is

$$y = (\mathbf{Z\Theta V w})\, x + n. \tag{7}$$

The ER is represented as

$$ER = \left(1 - \frac{T_E + T_F}{T}\right)\log_2\left(1 + \frac{|\mathbf{Z\Theta V w}|^2}{BN_0}\right). \tag{8}$$

B. Problem Formulation

In the single-user scenario, there is no interference from other users. Thus, $\mathbf{w}$ can be obtained by the maximum ratio transmission (MRT) beamforming

$$\mathbf{w} = \sqrt{p}\frac{(\mathbf{Z\Theta V})^H}{\|\mathbf{Z\Theta V}\|}. \tag{9}$$

The objective function (8) becomes

$$ER = \left(1 - \frac{T_E + T_F}{T}\right)\log_2\left(1 + \frac{p\|\mathbf{Z\Theta V}\|^2}{BN_0}\right). \tag{10}$$

T_E and T_F will proportionally reduce if the group size Q increases. But it will also lead to less flexibility of the RIS control. The choice of Q is based on the trade-off between the data transmission duration and the flexibility of RIS phase shift control.

Under the constraint of a limited P_{total} in (6), p might decrease if p_F increases, but $(T - T_E - T_F)$ will increase. Therefore, it is necessary to optimize transmit power allocation to balance the duration and rate of the data transmission.

With a given Q, we aim to maximize the ER by jointly optimizing the selection topology, phase shift design, and transmit power allocation. The problem is formulated as

$$\mathcal{P}1: \max_{p,p_F,\mathbf{Z},\mathbf{\Theta}} ER(p, p_F, \mathbf{Z}, \mathbf{\Theta}) \tag{11a}$$

$$\text{s.t. } C_1: P_{total} \le P_{max}, \tag{11b}$$

$$C_2: \| \mathbf{Z} \|_0 = M\rho, \tag{11c}$$

$$C_3: z_m \in \{0,1\}, \forall m = 1,2,\ldots,M, \tag{11d}$$

$$C_4: \theta_m \in \mathcal{F}, \forall m = 1,2,\ldots,M, \tag{11e}$$

where C_1 denotes the power constraint of the BS, C_2 and C_3 denote the irregular RIS constraints, and C_4 denotes the discrete valued phase shift constraint. Note that the objective function (10), the phase shift constraint C_2, and the irregular constraints C_3 and C_4 are non-convex.

III. Rate Optimization

To solve this problem, we can decouple the selection topology design $\mathbf{Z}$ from the other variables. Specifically, for a given topology $\mathbf{Z}$, $\mathcal{P}1$ can be reduced to

$$\mathcal{P}2: \max_{p,p_F,\mathbf{\Theta}} ER(p, p_F, \mathbf{\Theta}) \tag{12a}$$

$$\text{s.t. } C_1: P_{total} \le P_{max}, \tag{12b}$$

$$C_2: \theta_m \in \mathcal{F}, \forall m = 1,2,\ldots,M. \tag{12c}$$

Since the optimal $\mathbf{\Theta}$ is obtained by maximizing $\|\mathbf{Z\Theta V}\|^2$, the phase shift design is independent of p and p_F. Hence, the sub-problem $\mathcal{P}2$ can be solved by sequentially optimizing phase shift design and transmit power allocation. We use the adaptive tabu search (ATS) algorithm to optimize the selection topology. With a given topology $\mathbf{Z}$, $\mathbf{\Theta}$ in $\mathcal{P}2$ is solved by the alternating optimization (AO) technique. Then p and p_F are determined by the gradient descent method.

A. ATS-Based Irregular Topology Design

Exhaustively searching all possible topologies can obtain the optimal solution. However, it will also yield unrealistically high complexity because $\binom{M}{M_s}$ RIS topologies need to be traversed. Inspired by the tabu search algorithm, we propose the ATS algorithm in Algorithm 1 to optimize the topology of the irregular RIS. The ATS algorithm obtains a sub-optimal solution by iteratively searching the topology matrices according to an adaptive move criterion.

First, we initialize the selection topology $\mathbf{Z}_0$ by randomly selecting M_s ones and $(M - M_s)$ zeros. For the $\mathbf{Z}_{i-1}$ generated by the $(i-1)$-th iteration, we randomly swap q zeros and q ones of $\mathbf{Z}_{i-1}$ in the i-th iteration. Through this way, we can obtain o new matrices which are called the neighbors of $\mathbf{Z}_{i-1}$. To achieve a high-precision search, the neighbor distance q dynamically reduces as the number of iterations increases. A large q is selected at the beginning of iterations to achieve a wide search range.

To avoid redundant searches, we set a tabu list $\mathcal{H}$ to record the topology matrices that are searched in previous iterations.

Algorithm 1 ATS Topology Design Algorithm

Input: Tabu list $\mathcal{H}=\emptyset$, neighbor distance q, neighborhood size o, and number of iterations I_T.

Output: The selection topology $\hat{\mathbf{Z}}_{\text{opt}}$ and ER $\hat{R}_{\text{opt}}$.

1: Initialize the topology $\mathbf{Z}_0$ by randomly selecting M_s ones and $(M-M_s)$ zeros.
2: Obtain $\hat{\Theta}_{\text{opt}}$ by the AO technique, and then obtain $\hat{p}_F$ and $\hat{p}$ by the gradient descent method.
3: Calculate the ER R_0 and save $\hat{\mathbf{Z}}_{\text{opt}}=\mathbf{Z}_0$, $\hat{R}_{\text{opt}}=R_0$.
4: **for** $i=1,2,\cdots,I_T$ **do**
5: Update q according to the value of i. Randomly swap q zeros and q ones among the elements of $\mathbf{Z}_{i-1}$ and generate o neighbors.
6: Discard the neighbors already in $\mathcal{H}$ and add the rest into the tabu list $\mathcal{H}$.
7: Obtain phase shift design by the AO technique and then obtain transmit power allocation by the gradient descent method for the rest neighbors.
8: Calculate the ER for these neighbors and select the neighbor with the maximum ER as $\mathbf{Z}_i$. Update the $\hat{\mathbf{Z}}_{\text{opt}}$ and $\hat{R}_{\text{opt}}$.
9: **end for**

After excluding the neighbors that already exist in $\mathcal{H}$, we calculate the ER of the rest neighbors and select the one with the maximum ER as $\mathbf{Z}_i$. The neighbors in the i-th iteration are stored in the tabu list, and the globally optimal $\hat{\mathbf{Z}}_{\text{opt}}$ and $\hat{R}_{\text{opt}}$ are updated concurrently. Compared to exhaustive searching, ATS only searches $I_T o$ RIS topologies.

B. AO-based Phase Shift Design

Given a fixed $\mathbf{Z}$, the problem of optimizing $\mathbf{\Theta}$ is independent of p and p_F, which can be expressed as

$$\mathcal{P}3: \max_{\mathbf{\Theta}} \quad \|\mathbf{Z\Theta V}\|^2 \tag{13a}$$

$$\text{s.t.}\, C_1: \theta_m \in \mathcal{F}, \forall m=1,2,\ldots,M. \tag{13b}$$

An exhaustive search over all possible combinations of discrete phase shifts at selected groups incurs an exponential complexity of order $\mathcal{O}(2^{bM_s})$. Thus, we propose a low-complexity AO method to solve this problem.

Let $\mathbf{A}=\text{diag}(\mathbf{Z})\mathbf{V}(\text{diag}(\mathbf{Z})\mathbf{V})^H$. For a given m, fix $\theta_k, \forall k\neq m$. Then the objective function $\|\mathbf{Z\Theta V}\|^2$ is linear with respect to $e^{j\theta_m}$, which can be written as

$$2\text{Re}\Big\{e^{j\theta_m}\zeta_m\Big\}+\sum_{k\neq m}^{M}\sum_{i\neq m}^{M}\mathbf{A}_{k,i}e^{j(\theta_k-\theta_i)}+C, \tag{14}$$

where $\zeta_m=\sum_{k\neq m}^{M}\mathbf{A}_{m,k}e^{-j\theta_k}=|\zeta_m|e^{-j\varphi_m}$ and $C=\mathbf{A}_{m,m}$, with $\text{Re}\{\cdot\}$ denoting the real part of a complex number. The optimal continuous solution for the m-th element is $\theta_m=\varphi_m$. We round it to the nearest discrete value in $\mathcal{F}$ and then obtain the discrete solution

$$\hat{\theta}_m=\arg\min_{\theta\in\mathcal{F}}|\theta-\varphi_m|, \forall m. \tag{15}$$

By successively setting the phase shifts in the order of m based on (15), the objective value is non-decreasing. When the increase in $\|\mathbf{Z\Theta V}\|^2$ between consecutive iterations is below a predetermined threshold, we stop the iterations. To ensure the quality of the solution, we perform the AO method on multiple random initial matrices.

C. Transmit Power Allocation Design

Given $\mathbf{Z}$ and $\mathbf{\Theta}$, the ER becomes a function of p and p_F

$$ER(p,p_F)=\left(\frac{T-T_E}{T}-\frac{M+M_sb}{TB_F\log_2\left(1+\frac{p_F|h_F|^2}{N_0B_F}\right)}\right)\times\log_2\left(1+\frac{p\|\mathbf{Z\Theta V}\|^2}{BN_0}\right). \tag{16}$$

Maximizing the ER requires that C_1 in $\mathcal{P}2$ is satisfied as an equality, then $\mathcal{P}2$ becomes

$$\mathcal{P}4: \max_{p,p_F} ER(p,p_F) \tag{17a}$$

$$\text{s.t.}\, C_1: \frac{(T-T_E-T_F)}{T}p+\frac{p_FT_F}{T}=P_{max}. \tag{17b}$$

For any given p_F in C_1, a certain p can be calculated as

$$p=\frac{TP_{max}-p_FT_F}{(T-T_E-T_F)}. \tag{18}$$

Thus, the problem is transformed into a single-variable optimization problem about p_F. Next, we need to define the feasible region of p_F.

1) Lower Bound: According to (5), the reduction of p_F leads to an increase in T_F. It is required that $T_F<(T-T_E)$ to ensure the first two phases do not exceed the communication cycle duration. Through this constraint, we obtain the lower bound of p_F.

2) Upper Bound: When p_F increases to a certain value, p_FT_F will become an increasing function for p_F. To ensure that $p>0$ in (18), p_FT_F needs to be lower than the constant TP_{max}. The upper bound is also determined.

Based on the feasible region, the gradient descent method is utilized to optimize p_F. We execute iterations until the value of ER stabilizes. Then calculate the corresponding p according to (18).

IV. Numerical Results

In this section, we provide simulation results to evaluate the performance of the proposed irregular element-grouping RIS structure. Unless otherwise specified, the system parameters are given in Table I.

The irregular RIS has $N=192$ elements arranged in 12 rows and 16 columns. The path loss of the channel can be expressed as

$$\kappa=C_rd^{-\alpha}, \tag{19}$$

where d is the distance between the transmitter and the receiver, and Cr denotes the effect of channel fading and antenna gain. The parameters are set to $Cr=-30$ dB, $\alpha=2$,

TABLE I
SIMULATION PARAMETERS

Parameters	Values
Maximal average power of the BS P_{max}	30 dBm
Transmit power for channel estimation p_E	30 dBm
Bandwidth of the control feedback channel B_F	50 MHz
Bandwidth of the data transmission channel B	100 MHz
Noise power spectral density N_0	-174 dBm/Hz
Communication cycle duration T	15 ms
Spacing between adjacent elements	$\frac{\lambda}{8}$
Number of antennas at the BS K	2

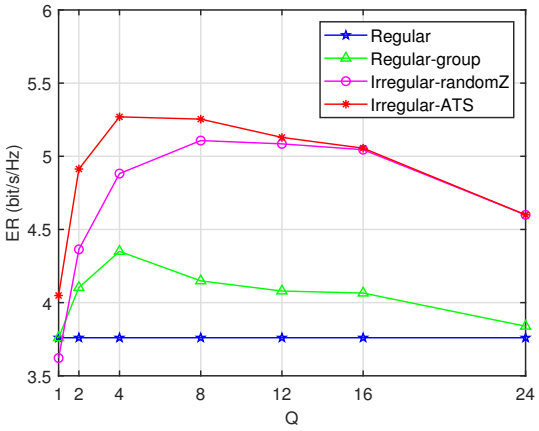

Fig. 4. ER versus the grouping size Q.

and $d = 15$ m for both the BS-RIS channel and the RIS-UE channel [15]. The parameters of the proposed Algorithm 1 are set to $o = 20$ and $I_T = 50$. All presented results have been averaged over 1000 independent realizations of the channel vectors $\mathbf{H}$, $\mathbf{G}$, and h_F.

For comparison, we consider the following schemes:

1) **Regular**: In this scheme, RIS is a regular surface consisting of $N\rho$ elements without grouping.
2) **Regular-group**: Based on 1), the element-grouping method is applied.
3) **Irregular-randomZ**: This scheme uses the proposed irregular element-grouping RIS structure. It groups N elements into M groups and selects $M\rho$ groups among them. Then randomly generate U topology matrices and choose the one with the largest ER.
4) **Irregular-ATS**: In contrast to 3), the topological matrix is obtained by the ATS algorithm.

Note that the four schemes utilize an equal number of elements. We set $U = I_T o$, thereby making the complexity of 3) consistent with that of 4).

Fig. 4 shows ER versus the grouping size Q when $\rho = 0.5$. The ER of 2), 3), and 4) outperforms that of 1). Because the element-grouping method saves time on channel estimation and control feedback. Thus, the increased duration of data transmission leads to a notable enhancement in the ER. The

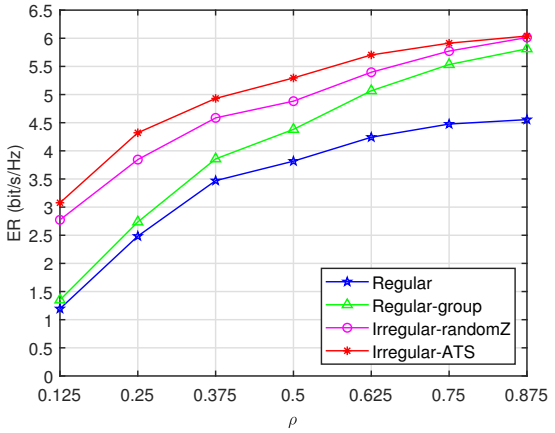

Fig. 5. ER versus the selected ratio ρ.

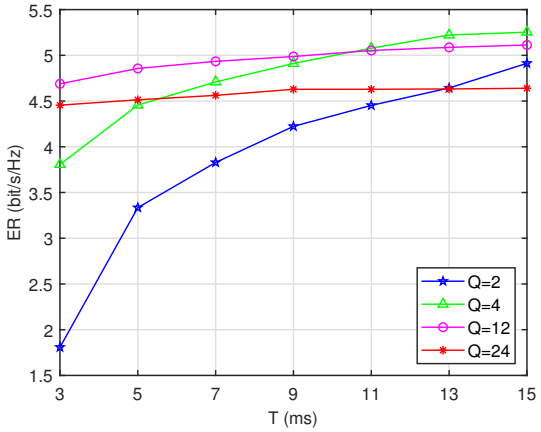

Fig. 6. ER versus the communication cycle duration T.

performance gap between 2) and 3), 4) demonstrates the superiority of the irregular structure. Due to the rational design of the ATS algorithm, the ER of 4) is larger than that of 3). It can be observed from Fig. 4 that the proposed structure achieves up to a 41% performance improvement compared to the regular RIS and up to a 24% performance improvement compared to the regular RIS with element-grouping. Moreover, the ER of 2), 3), and 4) exhibit a concave shape. This is because when Q is small, an increase in Q can significantly reduce T_F and T_E. As Q increases, the proportion of $(T_E + T_F)$ within T decreases, and the channel difference between the elements within one group becomes larger. A larger Q makes the phase shift control coarser, resulting in performance degradation.

Fig. 5 shows the ER versus the selected ratio ρ when $Q = 4$. From $\rho = 0.125$ to $\rho = 0.875$, the ER of scheme 1) increases by 2.8 times, while the ER of scheme 4) only increases by nearly 1 time. This indicates that the proposed structure is not sensitive to the value of ρ. Designing the topology through the ATS algorithm can utilize the elements that contribute more to the ER.

Moreover, the optimal grouping size Q is also dependent on the communication cycle duration T. Fig. 6 shows ER of the

scheme 4) versus T when $\rho = 0.5$. With the increase of T, ER experiences different levels of increase with different values of Q. Specifically, the increment of ER for lower Q is more prominent. This is because the time proportion of channel estimation and feedback control becomes smaller for a larger T, and the advantages brought by element-grouping become less significant. For large T, the precise control provided by small Q is more valuable. Thus, we can adjust the value of Q to accommodate changes in T when using the proposed structure.

V. Conclusion

In this paper, we proposed a novel irregular element-grouping structure under a practical transmission protocol. We selected the elements by designing the topology of irregular RIS and employed the element-grouping method to extend the data transmission duration. To maximize the ER, we designed a joint optimization algorithm. Specifically, we proposed an ATS algorithm to design the selection topology. With a given topology matrix, an AO method was introduced to optimize the phase shift design, and a gradient descent method was used to optimize the transmit power allocation.

The simulation demonstrated that compared to regular RIS and regular RIS with element-grouping, the proposed structure increased the ER by up to 41% and 24%, respectively. The numerical results also showed the strong adaptability of the proposed structure under different selected ratios and communication cycle durations.

References

[1] Q. Wu *et al.*, "Intelligent surfaces empowered wireless network: Recent advances and the road to 6G," *Proc. IEEE*, vol. 112, no. 7, pp. 724–763, Jul. 2024.

[2] Q. Wu, X. Guan, and R. Zhang, "Intelligent reflecting surface-aided wireless energy and information transmission: An overview," *Proc. IEEE*, vol. 110, no. 1, pp. 150–170, Jan. 2022.

[3] M. Hua, Q. Wu, W. Chen, O. A. Dobre, and A. L. Swindlehurst, "Secure intelligent reflecting surface-aided integrated sensing and communication," *IEEE Trans. Wireless Commun.*, vol. 23, no. 1, pp. 575–591, Jan. 2024.

[4] X. Yu, D. Xu, D. W. K. Ng, and R. Schober, "IRS-assisted green communication systems: Provable convergence and robust optimization," *IEEE Trans. Commun.*, vol. 69, no. 9, pp. 6313–6329, Jun. 2021.

[5] C. Pan *et al.*, "Multicell MIMO communications relying on intelligent reflecting surfaces," *IEEE Trans. Wireless Commun.*, vol. 19, no. 8, pp. 5218–5233, Aug. 2020.

[6] Q. Wu and R. Zhang, "Beamforming optimization for wireless network aided by intelligent reflecting surface with discrete phase shifts," *IEEE Trans. Commun.*, vol. 68, no. 3, pp. 1838–1851, Mar. 2020.

[7] X. Yu, D. Xu, and R. Schober, "Optimal beamforming for MISO communications via intelligent reflecting surfaces," in *Proc. IEEE SPAWC*, May. 2020, pp. 1–5.

[8] E. Björnson, Ö. Özdogan, and E. G. Larsson, "Intelligent reflecting surface versus decode-and-forward: How large surfaces are needed to beat relaying?" *IEEE Wireless Commun. Lett.*, vol. 9, no. 2, pp. 244–248, Feb. 2020.

[9] H. Zhang, B. Di, Z. Han, H. V. Poor, and L. Song, "Reconfigurable intelligent surface assisted multi-user communications: How many reflective elements do we need?" *IEEE Wireless Commun. Lett.*, vol. 10, no. 5, pp. 1098–1102, May. 2021.

[10] D. Li, "Ergodic capacity of intelligent reflecting surface-assisted communication systems with phase errors," *IEEE Commun. Lett.*, vol. 24, no. 8, pp. 1646–1650, Aug. 2020.

[11] A. Zappone, M. Di Renzo, F. Shams, X. Qian, and M. Debbah, "Overhead-aware design of reconfigurable intelligent surfaces in smart radio environments," *IEEE Trans. Wireless Commun.*, vol. 20, no. 1, pp. 126–141, Jan. 2021.

[12] E. Björnson and L. Sanguinetti, "Rayleigh fading modeling and channel hardening for reconfigurable intelligent surfaces," *IEEE Wireless Commun. Lett.*, vol. 10, no. 4, pp. 830–834, Apr. 2021.

[13] P. Rocca, G. Oliveri, R. J. Mailloux, and A. Massa, "Unconventional phased array architectures and design methodologies—A review," *Proc. IEEE*, vol. 104, no. 3, pp. 544–560, Mar. 2016.

[14] B. Zheng and R. Zhang, "Intelligent reflecting surface-enhanced OFDM: Channel estimation and reflection optimization," *IEEE Wireless Commun. Lett.*, vol. 9, no. 4, pp. 518–522, Jul. 2020.

[15] Z. Zhang and L. Dai, "A joint precoding framework for wideband reconfigurable intelligent surface-aided cell-free network," *IEEE Trans. Signal Process.*, vol. 69, pp. 4085–4101, Apr. 2021.